



Preparation of N-TiO₂/PbS Nanocomposite Using Successive Ionic Layer Adsorption and Reaction (SILAR) Method

ANTI KOLONIAL PRODJOSANTOSO*, NIKMAHTUL EVIANA,
CAHYORINI KUSUMAWARDANI and KRISTIAN HANDOYO SUGIYARTO

Department of Chemistry, Yogyakarta State University, Yogyakarta 55281, Indonesia.

*Corresponding author E-mail: prodjosantoso@uny.ac.id

<http://dx.doi.org/10.13005/ojc/340523>

(Received: August 29, 2018; Accepted: September 10, 2018)

ABSTRACT

Titanium oxides are well known semiconductor and have been studied intensively in term of their physical and chemical properties, and also the applications. The oxides have been modified in many ways to improve the catalytic capability. Nitrogen has been doped and dyes have been introduced into TiO₂. N-TiO₂/PbS nanocomposite has been synthesized using successive ionic layer adsorption and reaction (SILAR) method, by which ITO glass layered with N-TiO₂ was immersed several cycles in a homogenous mixture of Pb(CH₃COO)₂ and (NH₄)₂S. The combination method of XRD, UV-Vis, and SEM have been used to characterize the samples. It is confirmed that N-TiO₂/PbS exists in the samples. The particle size of PbS is about 6-8 nm. The UV-Vis study reveals that the Eg₁ of N-TiO₂/PbS is lower than that of Eg of N-TiO₂ itself, and the Eg₂ ie. about 1.62 eV.

Keywords: Nanocomposite, Solar cell, PbS, SILAR.

INTRODUCTION

Solar energy, a clean, non-polluting, safe, and unlimited energy, has been proposed to alternatively replace the nonrenewable energy sources, such as coal and oil.¹ The availability of solar energy in the form of sunlight received by the earth's surface is much more than enough to cover the energy consumed by the entire world today.² However, we need an efficient photovoltaic technology using semiconductor devices called solar cells for converting the sunlight directly into electrical energy.³

In the last few decades, for example,

the titanium oxide (TiO₂) has been enormously studied. Although TiO₂ is very promising, there are still shortcomings. The pure TiO₂ can only be activated under UV light irradiation ($h\nu < 390$ nm) because of its large band gap energy (3-3.4 eV). In order to extend the light absorption edge to visible region, many attempts have been undertaken.⁴ A combination of organic-inorganic nanostructure semiconductor has been attempted to prepare superior solar cells.^{5,6} The dye-sensitized solar cell (DSSC) based on titanium dioxide (TiO₂) having an efficiency of 11% has also been applied for the solar cell.⁷ Asahi *et al.*, succeeded in increasing the visible light absorption properties of TiO₂ semiconductors



through nitrogen deposition.⁸ The addition of N to the TiO₂ framework results in a band gap narrowing caused by the overlapping of the N 2p with the O 2p orbitals. Furthermore, the use of N-TiO₂ materials can improve the efficiency and stability of solar cells.^{9,10} However, the more stable compounds such as CdS, CdSe, PbS, and InAs have been proposed to prepare semiconductors.¹¹ In this study, PbS was introduced to the N-TiO₂ material by successive ionic layer adsorption reaction (SILAR) method, to prepare N-TiO₂/PbS nanocomposite.

MATERIALS AND METHODS

Materials. Titanium tetraisopropoxide (TTIP) (Merck 97%), ethylenediamine (Merck ≥99%), (NH₄)₂S (Merck ≥ 20%), Triton-X (Merck), Pb(CH₃COO)₂·3H₂O (Merck ≥99,5%), acetyl acetic acid (Merck 100%), and ITO glass substrates (Dyesol) have been used as received without any prior treatments.

Methods. X-ray powder diffraction (XRD) analysis was carried out using XRD Rigaku Miniflex 600 with Cu K α radiation ($\lambda=1.5405981$ Å), operated at 40 kV and 30 mA. Scanning electron microscopy (SEM) measurement was performed on SEM JEOL JED-2300. UV-Vis diffuse reflectance spectra (DRS) were determined by a UV-Vis UV 1700 Pharmaspec Spectrophotometer Specular Reflectance Attachment.

Synthesis of N-TiO₂ NPs

The N-TiO₂ NPs was synthesized using the method developed by Kusumawardani *et al.*,¹² A quantity of 6.7 mL ethylenediamine was dissolved in 80 mL of absolute ethanol and stirred for 2 h to obtain homogeneous solution. 3 mL TTIP was added dropwise into the solution while stirring for 1 hour. The resulted homogeneous solution was refluxed at 80° C for 6 h and then cooled to room temperature, and added with 15 mL glacial acetic acid. Hydrolysis was carried out with the addition of 21.6 mL of demineralized water dropwise followed by stirring for 24 hours. The smixture was allowed to stand for 24 h and the yellow solids obtained was filtered off. The solid was dried at 80°C for 8 h and calcined at 450°C for 4 h with heating rate of 2°C per min. to produce the N-TiO₂ NPs powder.

The N-TiO₂ thin layer was prepared on ITO glass substrates of 2.5 x 1.5 cm². A 2 g of N-TiO₂ powder was thoroughly mixed with 0.05 mL of triton-X and 0.01 mL acetyl acetone to produce a paste which was then deposited onto the glass substrate surface by the doctor blade technique,¹³ and calcined at 400°C for 2 hours.

Preparation of N-TiO₂/PbS was carried out by applying Pb²⁺ and S₂₋ ions on the N-TiO₂ substrate. The N-TiO₂ substrate was preheated using an oven at 60°C for 10 min. and immersed varies between 1, 5, 15, 25, and 50 cycles for 10 sec. each into a mixture of 0.2 M of Pb(CH₃COO)₂ and 0.4 M of (NH₄)₂S solutions, and finally air dried.

RESULTS AND DISCUSSION

N-TiO₂/PbS nanocomposite has been prepared using a successive ionic layer adsorption and reaction (SILAR) method with 1, 5, 15, 25, and 50 cycle's variation. The powder XRD patterns of N-TiO₂/PbS nanocomposites, ITO, PbS and N-TiO₂ materials can be seen in Fig. 1. In general, the XRD patterns of N-TiO₂/PbS nanocomposites indicate the presence of TiO₂ (anatase), ITO and PbS phases. The line at 2 θ about 26.20° indicates the TiO₂ (anatase) (Fig. 1.b to 1.g), performing that the character of TiO₂ still remains after the immersion processes. The surface of N-TiO₂ layered by PbS could be recognized by the presence of selected but characteristic diffractogram of PbS at 2 θ about 30.15° (Fig. 1.b to 1.h). The stronger peak relates to the more immersion the N-TiO₂ into the Pb²⁺ and S₂₋ solution, and so the more PbS adsorbed onto the surface of N-TiO₂. Despite the strong intensity may be resulted by the high crystallinity of PbS. A selected peak in the red-dashed box (Fig. 1.b) indicates the absence of PbS from unimmersed sample. Some strong peaks of ITO are also observed at 2 θ about 27.23°, 34.42°, and 38.48°, and 52.23°.

The XRD of PbS consists of planes (111), (200), (220), (311), and (222).^{14,15} The XRD spectra of N-TiO₂/PbS one cycle shows no peaks of PbS, but only TiO₂ and ITO. This is probably occurred as only very little amount of PbS is adsorbed on the surface of N-TiO₂. The PbS spectra are observed at XRD pattern of N-TiO₂ 5 cycle. However, the spectra are weak and are not clearly visible. This may be

due to improper crystal orientation, so that when the crystal is subjected to X-rays, many of the diffracted rays out of the detector. Observable PbS spectra are seen in the N-TiO₂/PbS spectra of 15, 25, and 50 cycles (Figure. 1. e-1.g).

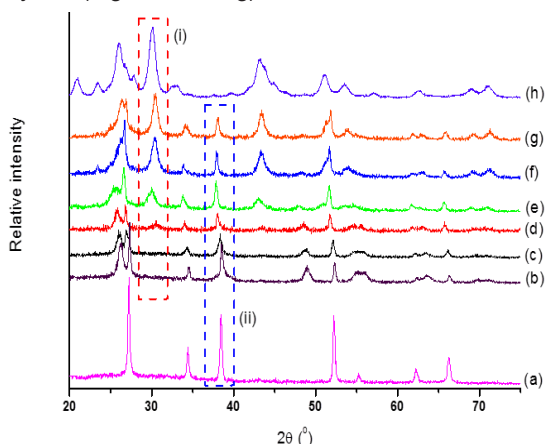


Fig. 1. Powder XRD patterns of ITO (a), N-TiO₂/PbS with 0 (b), 1 (c), 5 (d), 15 (e), 25 (f), and 50 cycles (g), and PbS (h)

The size of PbS crystallite over the N-TiO₂ can be determined from the broadening of corresponding X-ray spectral peak by Scherrer formula¹⁶

$$D = \frac{0,9 \lambda}{\beta \cos \theta}$$

Where D is crystallite size (nm), k is a material constant (0.9), λ is the X-ray wavelength used for the measurement (nm), β is the selected peak FWHM. The PbS crystallite sizes are listed in Table 1. The crystallite size of PbS material is ranged from 6.05 nm to 8.07 nm (Table 1). This is in agreement with Popa *et al.* stating that the size of PbS crystallite is between 5 to 20 nm.¹⁷

Tabel 1: Crystallite size of PbS over the N-TiO₂

Cycle variation (time)	Crystallite size (nm)
5	7.51
15	7.84
25	8.07
50	6.05

The UV-Vis diffuse reflectance spectra of the N-TiO₂/PbS samples are shown in Fig. 2. Obviously, the UV-Vis adsorption edge of N-TiO₂/PbS shifts to the visible-light region along with the more immersion cycles. The absorbance of the PbS-sensitized N-TiO₂ samples is not proportional to the number of immersion cycles, although at the time of immersion the formation of

black color of the PbS was getting darker along with the number of immersions. The resulting absorbance value is depend on the non-uniform particle size of N-TiO₂/PbS absorbing light with different energy.

Furthermore, N-TiO₂/PbS samples indicate two characteristic light absorption edges. The first absorption edge corresponds to the electron promotion from the valence to the conduction bands, while the other originates from the new energy levels in the forbidden band of TiO₂ formed by N-doping.

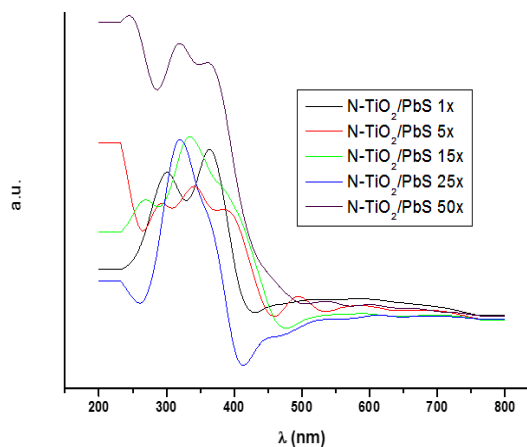


Fig. 2. The UV-Vis spectra of N-TiO₂/PbS

The N-TiO₂ gives only the absorption value in the UV region (λ <375 nm). Whilst the N-TiO₂/PbS systems indicate absorption shifting towards the visible light. This increases the optical absorption intensity due to the sensitization of PbS on the N-TiO₂, and the absorptions undertake at wavelengths greater than 400 nm. The N-TiO₂/PbS provides the change of electronic transition to the UV region as well as to the visible light (Table 2).

The changes of electronic transition occur in UV and visible areas. The samples of N-TiO₂/PbS immersed 5,15, and 50 cycles provide the maximum absorbances of 294 nm, 270 nm, and 244 nm, respectively, indicating intraligand transitions π→π*. Intraligand transitions π→π* occurred due to the presence of nitrogen atoms in TiO₂ lattices. According to Asahi *et al.*, the doped nitrogen in the TiO₂ matrix can alter the structure of the electronic band of titania by combining the 2p nitrogen and 2p oxygen (N 2p and O 2p → Ti d_{xy}) orbitals, thus shortening the bandgap energy of the TiO₂ material significantly.^{8,18} The presence of the intraligand transition π→π* indicates that nitrogen is being doped in TiO₂.

Table 2: Absorbances the N-TiO₂/PbS

Sample	λ Visible (nm)	λ UV (nm)	$d-d$ (nm)	$\pi \rightarrow \pi^*$ (nm)
N-TiO ₂ /PbS (1x)	525	363, 301	363	-
N-TiO ₂ /PbS (5x)	495	294, 340	340	294
N-TiO ₂ /PbS (15x)	588	270, 334	334	270
N-TiO ₂ /PbS (25x)	613	320	320	-
N-TiO ₂ /PbS (50x)	536	244, 319	319	244

The N-TiO₂/PbS immersed by 1, 5, 15, 25, and 50 cycles show the maximum absorbances of 363 nm, 340 nm, 334 nm, 320 nm, and 319 nm, respectively, indicating an overlapping metal-ligand charge transfer (MLCT) electronic transition ($d \rightarrow d$ transition). The samples also show several electronic transitions in visible light areas giving the maximum absorbances of 525 nm, 495 nm, 588 nm, 613 nm, and 536 nm, which also indicate a MLCT.^{19,20}

plotting $[F(R'_{\infty}) \cdot h\nu]^{1/2}$ versus energy of light.^{21,22} The selected graphs are presented in Fig. 3a and 3b. The band gap energies of the samples are tabulated in Table 3. The band gap energies are 2.14 and 3.49 eV, and 3.50 eV for N-TiO₂ and TiO₂, respectively, revealing that the band gap of TiO₂ was narrowed by N doping. In this work, the band gap narrowing may be caused by the introduction of nitrogen from ethylenediamine into the lattice of TiO₂. Therefore, it can be concluded that the sample of N-TiO₂ may exhibit high photocatalytic activity under visible-light irradiation.^{23,24}

The Kubelka–Munk function was used to calculate the band gap energies of the samples by

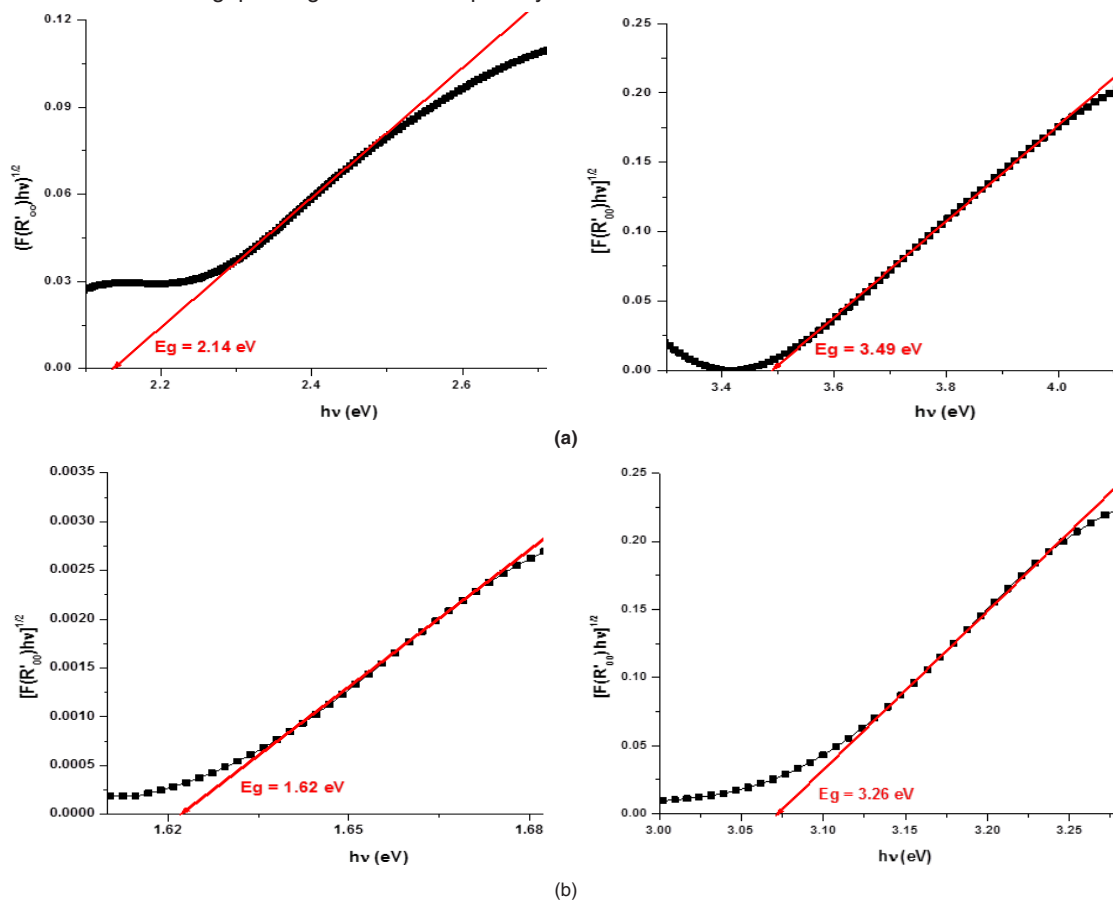


Fig. 2. Bandgap energy of (a) N-TiO₂, and (b) N-TiO₂/PbS 15 immersion cycles

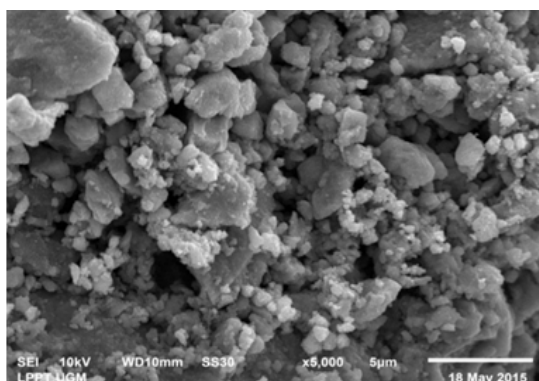
The band gap energies of the N-TiO₂/PbS are listed in Table 3. The pure N-TiO₂ material produces two band gap energies of about 2.14 eV (Eg₁) and 3.49 eV (Eg₂) while the N-TiO₂/PbS has Eg₁ and Eg₂ about 1.63 eV and 3.07 eV, respectively. The Eg₁ is steady along with the increasing of cycles, while Eg₂ decreases. A significant decrease of Eg₂ occurs after sensitization of the N-TiO₂ thin layer

using PbS. The PbS sensitization of TiO₂ thin layer also increases the device voltage by pressing the thin layer TiO₂ surface.^{25,26} Increasing the device voltage will decrease the distance between the conduction band gap and the valence band.

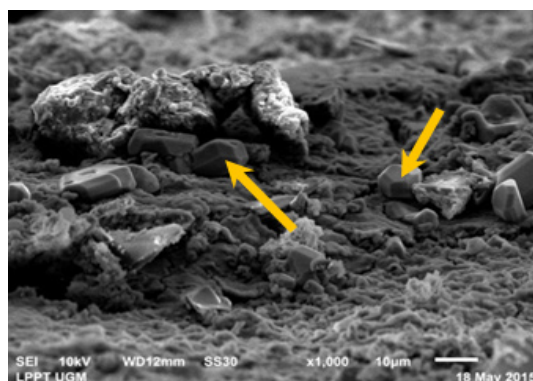
Table 3: Band gap energies of N-TiO₂/PbS

Samples	Band gap energy (eV)	
	Eg ₁	Eg ₂
TiO ₂ (anatase)	-	3.50
N-TiO ₂	2.14	3.49
N-TiO ₂ /PbS (1 cycle)	1.64	3.07
N-TiO ₂ /PbS (5 cycles)	1.63	3.07
N-TiO ₂ /PbS (15 cycles)	1.63	3.07
N-TiO ₂ /PbS (25 cycles)	1.63	3.04
N-TiO ₂ /PbS (50 cycles)	1.63	2.78

Characterization using the SEM method was performed to study the morphology of N-TiO₂ and N-TiO₂/PbS samples. The pure N-TiO₂ consists of irregular shape particles with sizes of 1 to 2.5 μm (Fig. 4.a). The N-TiO₂/PbS samples indicate two different morphologies, ie. irregular and regular in shapes. The existence of regular shaped particles allegedly as PbS are more dominant in sample with more cycles. The SEM micrograph of N-TiO₂/PbS with 50 cycles can be seen in Fig. 4. b. The sample consists of irregular shaped particles with the size varies between 1 to 2.5 μm, and the regular shaped having size of about 5 μm.



(a)



(b)

Fig. 3. SEM micrographs of N-TiO₂ (a) and N-TiO₂/PbS 50 cycles (b). Yellow arrows are pointing regular shape particles which could be allegedly as the crystalline PbS

CONCLUSION

The N-TiO₂ PbS crystallites have the size of about 6.05-8.06 nm, dominated by the structures of N-TiO₂ anatase and PbS cubic. The immersion

cycles of N-TiO₂ in the PbS deposition solution do not significantly affect the band gap energies, however the PbS sensitization to the N-TiO₂ by the SILAR method decreases the band gap energies.

REFERENCES

- International Renewable Energy Agency (IRENA), *Technology Roadmap.*, **2018**.
- Chwieduk, D., *Solar Energy in Buildings.*, **2014**, 21, 62.
- Sampaio, P. G. V.; Gonzalez, M.O.A., *Renew. Sustain. Energy Rev.*, **2017**, 74, 590-601.
- Español, P.; Serrano, M.; Pagonabarraga, I; Zúñiga, I., *Soft Matter.*, **2016**, 12, 4821-4837.
- Kim, Y.H.; Kwon, S.G.; Sung, M. J. *Repub. Korean Kongkae Taeho Kongbo.*, **2017**, -, 28.
- Xu, W.; Tan, F.; Liu, X.; Zhang, W.; Qu, S.; Wang, Z.; Wang, Z., *Nanoscale Res. Lett.*, **2017**, 12, -.
- Son, D.-Y.D.D.-Y.D.D.-Y.; Im, J.-H.J.J.-H.J.; Kim, H.-S.H.; Park, N.-G.N.N.-G., *J. Phys. Chem. C.*, **2014**, 118, 16567-16573.
- Asahi, R.; Ohwaki; Taoki; Ktaga, Y., *Science.*, **2001**, 293, 269-271.

9. Zhang, Z.-L.; Li, J.-F.; Wang, X.-L.; Qin, J.-Q.; Shi, W.-J.; Liu, Y.-F.; Gao, H.-P.; Mao, Y.-L., *Nanoscale Res. Lett.*, **2017**, *12*, 43.
10. Kushwaha, R; Chauhan, R.; Srivastava, P.; Bahadur. L., *J. Solid State Electrochem.*, **2015**, *19*, 507-517.
11. Liu, J.; Gao, C.; Luo, L.; Ye, Y.Q.; He, X.; Ouyang, L.; Guo, X.; Zhuang, D.; Liao, C.; Mei, J.; Lau, L.; Woon, M., *J. Mater. Chem. A.*, **2015**, *3*, 28-30.
12. Kusumawardani, C. Private communication, 2018
13. Wang, Y.; Li, J.; Xue, C.; Zhang, Y.; Jiang, G.; Liu, W.; Zhu, C., *Electron. Mater. Lett.*, **2017**, *13*, 478-482.
14. Mamiyev, Z.Q.; Balayeva, N.O., *Opt. Mater. (Amst)*, **2015**, *46*, 522-525.
15. Suganya, M.; Balu, A.R., *Mater. Sci.*, **2017**, *35*, -.
16. Smilgies, D.-M. *J. Appl. Crystallogr.*, **2009**, *42*, 1030-1034.
17. Popa, A.; Lisca, M.; Stancu, V.; Buda, M.; Pentia, E.; Botila, T., *Journal of Optoelectronics and Advanced Materials.*, **2006**, *8*, 43-45.
18. Asahi, R.; Morikawa, T., *Chem. Phys.*, **2007**, *339*, 57-63.
19. Wang, S.; Yu, Z.C.; Han, L.; Dai, C.L.; Song, J.Y., *Asian J. Chem.*, **2012**, *24*, 214-216.
20. Harris, J.A.; Trotter, K.; Brunschwig, B.S., *J. Phys. Chem. B.*, **2007**, *111*, 6695-6702.
21. Lin, H.; Huang, C.P.; Li, W.; Ni, C.; Ismat, S.S.; Tseng, Y.-H., *Appl. Catal. B Environ.*, **2006**, *68*, 1-11.
22. Ahsan, R.; Khan, M.Z.R.; Basith, M.A., *J. Nanophotonics.*, **2017**, *11*, -.
23. Liu, C.; Zhang, L.; Liu, R.; Gao, Z.; Yang, X.; Tu, Z.; Yang, F.; Ye, Z.; Cui, L.; Xu, C.; Li, Y., *J. Alloys Compd.*, **2016**, *656*, 24-32.
24. Tang, R.; Jiang, Q; Liu, Y., *Procedia Eng.*, **2017**, *205*, 573-580.
25. Cai, F.; Yang, F.; Zhang, Y.; Cai, F.; Yang, F.; Zhang, Y.; Ke, C.; Cheng, C.; Zhao, Y.; Yan, G., *Phys. Chem.*, **2014**, *16*, 23967-23974.
26. Basit, M.A.; Abbas, M.A.; Jung, E.S.; Park, Y.M.; Bang, J.H.; Park, T.J. *Electrochim. Acta.*, **2016**, *211*, 644-651.